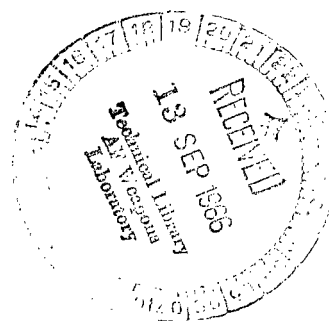**NASA TECHNICAL NOTE**

NASA TN D-3354

A VISUAL STUDY OF VELOCITY
AND BUOYANCY EFFECTS
ON BOILING NITROGEN

by Robert J. Simoneau and Frederick F. Simon

Lewis Research Center
Cleveland, Ohio

NASA TN D-3354

A VISUAL STUDY OF VELOCITY AND BUOYANCY

EFFECTS ON BOILING NITROGEN

By Robert J. Simoneau and Frederick F. Simon

Lewis Research Center
Cleveland, Ohio

NATIONAL AERONAUTICS AND SPACE ADMINISTRATION

A VISUAL STUDY OF VELOCITY AND BUOYANCY
EFFECTS ON BOILING NITROGEN

by Robert J. Simoneau and Frederick F. Simon

Lewis Research Center

SUMMARY

A visual study of the nucleate and film-boiling regimes of liquid nitrogen was con-
ducted. The test section was a vertical channel heated from one side and operated at low
velocity. Nitrogen was caused to flow either upward or downward to evaluate the buoy-
ancy orientation effect on the hydrodynamics of boiling.

A strong body-force orientation effect was noted in both boiling regimes at a low ve-
locity of 0.85 foot per second; the effect was reduced at a higher velocity of 3.5 feet per
second. The buoyancy effect primarily affects vapor accumulation and bubble trajectory.
This, in turn, influences the critical heat flux.

An instability of the vapor-liquid interface, analogous to wave formation on a liquid
surface by a gas stream, was noted in film boiling. This visual result supports the use
of the Helmholtz-Kelvin stability criterion for film boiling. Measurements of the film
thickness h_{min} and the most unstable wavelength λ_{us} at the onset of instability indi-
cated that the following relation exists for liquid nitrogen:

$$\lambda_{us} = 4 \, h_{min}$$

INTRODUCTION

The research tool that has led to much insight into boiling mechanisms is the visual
experimental study. In these experiments, heat-transfer data are taken simultaneously
with high-speed motion pictures of the flow patterns in an effort to establish a model.
This can be accomplished in forced convection by the use of a heated glass tube (refs. 1
and 2). This technique yields a realistic flow model, but the tube curvature makes in-
vestigation of the boiling activity at the heated surface difficult. In addition, high vapor
generation can obscure the two-phase flow within the tube. What is needed for ideal

photographic conditions is less heated area to permit a better overall view of the two-phase hydrodynamics and detailed inspection of the boiling mechanism at the heated surface. A flat heating surface was used to obtain the ideal photographic conditions reported in references 3 to 5. This method is used herein, although geometric realism is sacrificed for the sake of visual advantage.

The results of a photographic and data study of boiling liquid nitrogen flowing at low velocity through a channel with a square cross section heated from one side and with glass windows on opposite sides are presented. The facility was constructed so that the nitrogen could flow either upward or downward. Thus, it was possible to examine both velocity and body-force orientation effects on the boiling processes. The results of the interaction of velocity and body-force orientation are focused on the region near the critical heat flux and on the film-boiling regime. In addition to the body-force and velocity effects, visual results on film-boiling instability are reported.

A motion picture supplement C-245 is available on loan. A request card and a description of the film are given at the back of this report.

APPARATUS AND PROCEDURE

Flow System

The basic flow facility was a blowdown type, as illustrated in figure 1. Liquid nitrogen was forced into the flow system from the 500-gallon (1890-liter) supply Dewar by using nitrogen gas from a self-pressurizing bleed system. The flow rate was monitored by a venturi and was controlled by a throttle valve upstream of the test section. The test-section pressure was maintained by a second throttle-pressure-regulating valve downstream of the test section. The liquid was then vented to the atmosphere. The large-capacity supply Dewar allowed continuous operation for at least 3 hours; thus, the entire system could be cooled to liquid-nitrogen temperature. The primary flow direction was upward, as shown in figure 1. The variation in buoyancy-force orientation was achieved merely by reversing the control valves and piping so that the nitrogen flowed downward.

The test section was enclosed in a vacuum chamber to keep the windows from frosting. The vacuum chamber had acrylic resin windows in front and in back so that the test section could be viewed completely.

Test Section

The test section was a 1- by 1-inch (1 in. = 0.0254 m) flow chamber with borosilicate
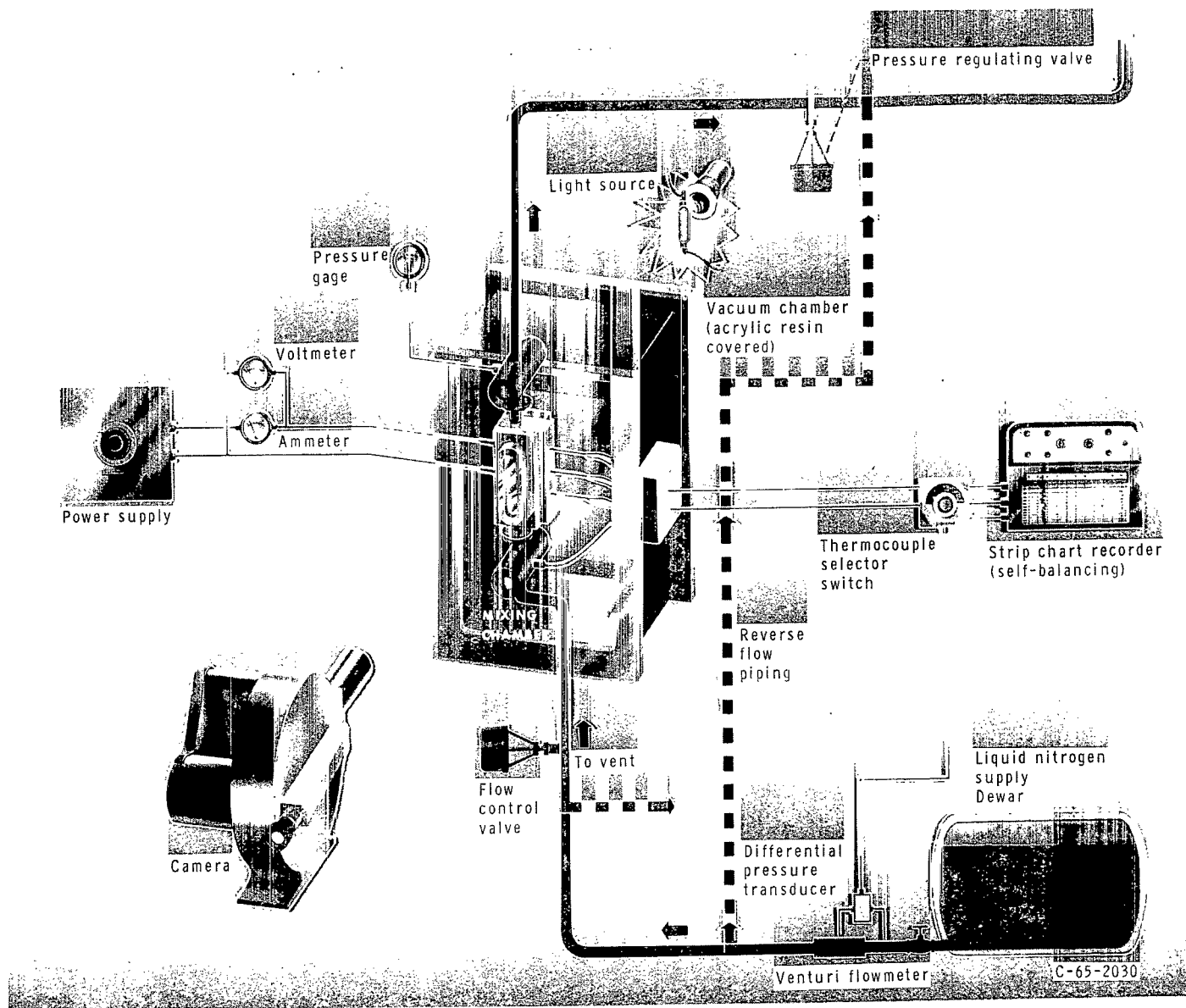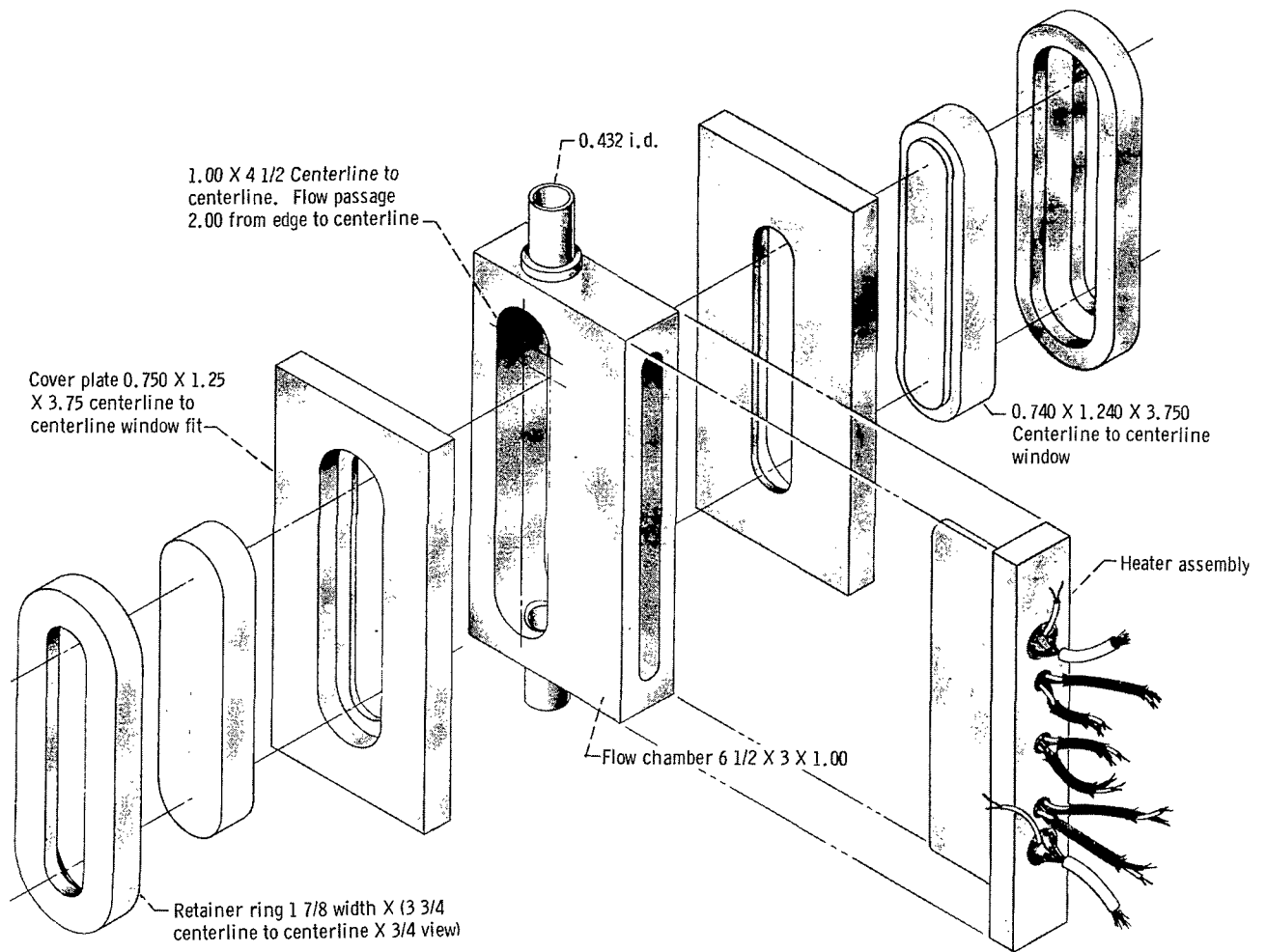
Figure 1. - Experimental facility.

Pressure regulating valve

Light source

Pressure gage

Voltmeter

Ammeter

Power supply

Vacuum chamber (acrylic resin covered)

Thermocouple selector switch

Strip chart recorder (self-balancing)

Reverse flow piping

Camera

To vent

Flow control valve

Liquid nitrogen supply Dewar

Differential pressure transducer

Venturi flowmeter

C-65-2030

3

1.00 X 4 1/2 Centerline to centerline. Flow passage 2.00 from edge to centerline

0.432 i.d.

Cover plate 0.750 X 1.25 X 3.75 centerline to centerline window fit

0.740 X 1.240 X 3.750 Centerline to centerline window

Heater assembly

Flow chamber 6 1/2 X 3 X 1.00

Retainer ring 1 7/8 width X (3 3/4 centerline to centerline X 3/4 view)

CD-8518

Figure 2. - Test section assembly. (All dimensions are in inches.)

glass windows mounted in cover plates in front and in back (fig. 2). The heating surface was mounted on a phenolic resin block inserted from the side. This mounting allowed the use of various heater configurations in the same flow channel. A careful examination of figure 2 reveals an important point concerning the views shown in the succeeding photographs. The oblong windows are located so that the center of the window is over the right edge of the flow passage to ensure a good view of the heated surface The view is therefore 1/2 inch wide, and the left half of the channel is not visible in the photographs. For a higher velocity, an insert was placed in the flow passage for some runs. The insert blocked out three-fourths of the channel, which increased the velocity by a factor of 4. Since this insert blocked the left three-fourths of the passage, the view in the photographs with the insert was that of the entire flow channel.

4

(a) Heater A.

(b) Heater B (assembly same as A except that B has no heat loss thermocouples).

Figure 3. - Heater strip. (All dimensions are in inches.)

CD-8519

Two heater configurations were used and are shown in detail in figure 3. Heater A was an iron-chromium-aluminum alloy strip mounted flush on the phenolic resin block. The block protruded 1/16 inch into the channel. This test section had the better hydrodynamic configuration, and the flow can be considered similar to flow over a flat plate. Therefore, the data from this heater are considered to be more reliable. Heat losses were calibrated and subtracted from the data. Because the heater was mounted flush with the wall, it is difficult to locate the position of the heated surface in the photographs.

5

For a more detailed study of processes at the surface, a thin heater strip, heater B, of the same material as heater A was placed in the mainstream. In this condition, free from the phenolic resin block, a good edge view of the heater strip was obtained.

Instrumentation

The power supply for the heater strip was a 60-cycle 30-ampere variac. The maximum power requirement was about 150 watts. The power was measured by an alternating current voltmeter and ammeter. The pressure drop across the venturi was measured with a strain gage differential transducer, and the signal was displayed on a self-balancing potentiometric strip-chart recorder. All temperatures were measured with Chromel-constantan thermocouples fed by a manual switch to the strip-chart recorder. The bulk pressure was monitored on a Bourdon gage.

Photographic Equipment

Two methods of photography were used, still pictures and high-speed motion pictures. The same lighting arrangement was used for both photographic systems. Photographs were taken from the front with the light located directly to the rear, as illustrated in figure 1 (p. 3). For the still pictures, the light was dispersed by a ground glass screen between the light and test section.

The high-speed motion pictures were taken at a nominal speed of 5000 frames per second. A 60-cycle timing light was used to mark the film for speed. A 2-inch focal-length lens was used for the overall views of heater A. For the detailed closeups of heater B, a 6-inch focal-length lens was used. The light source was a 1000-watt tungsten filament lamp. The still pictures were taken with a 4 by 5 press camera and a strobe light.

Procedure

The system was purged of all moisture first. Liquid nitrogen was then passed through until all components were at liquid-nitrogen temperature, and the flow rate was set. All tests were run at a pressure of 35 pounds per square inch absolute (2.41×10^5 N/m^2); thus, the inlet bulk fluid was approximately 6° to 10° R (3° to 6° K) subcooled. The exit was always subcooled. Data were taken at various steady power levels. At each power level, flow, power, and temperature data were recorded, and either a motion

picture or a still photograph was taken. The normal procedure was to move up to the critical heat flux in power, record the point, and then reduce the power to the minimum film-boiling level.

Power was determined from voltage and amperage measurements. The strip resistance was measured and served as a check of the power input. The heat flux for heater A was corrected for heat loss by calibrating the heat flow to the chamber walls as a function of temperature difference between the strip and the chamber.

Accuracy

The errors in temperature are at least 3° to -8° R (2° to -5° K). This error is a result of recording accuracy and thermal electromotive forces in the leadout junction through the vacuum chamber walls. An additional error is possible because of alternating-current pickup across the thermocouple junction. These errors prevented accurate temperature data in the nucleate-boiling region. The percent error in the film-boiling region is much less than it is in the nucleate-boiling region; but, because of the uncertainty of the magnitude of the alternating-current pickup, the reliability of the film-boiling temperatures is subject to question. The main value of the temperature lies in the determination of the onset of film boiling at the critical heat flux and the onset of nucleate boiling of the minimum heat flux. The power was measured to within 8 percent. The remaining measurements were well within 5 percent.

BOILING CURVE OF HEATER A

As an introduction to the data and photographs, an overall look should be taken at the complete range of boiling conditions attainable. This phenomenon is shown graphically and photographically for upward flow in figures 4 and 5.

The data in figure 4 are plotted against the pool-boiling curve of reference 6 as a reference condition. The nucleate-boiling temperatures are shown with uncertainty limits because of measurement errors. The three velocity conditions shown are 0.80, 1.1, and 3.4 feet per second (1 ft/sec = 0.3048 m/sec).

The photographs in figure 5 were taken at a velocity of 0.80 foot per second, and the conditions for each photograph are indicated in figure 4. Figure 5 represents a normal progression through the boiling cycle, as described in the section Procedure. Figures 5(a) to (c) represent an increasing power application toward the critical heat flux. The heat-flux levels are approximately 20, 70, and 85 percent of the critical heat flux, as shown in figures 5(a), (b), and (c), respectively. The first observation that might be made is the tremendous increase in vapor mass with power. The small (less than
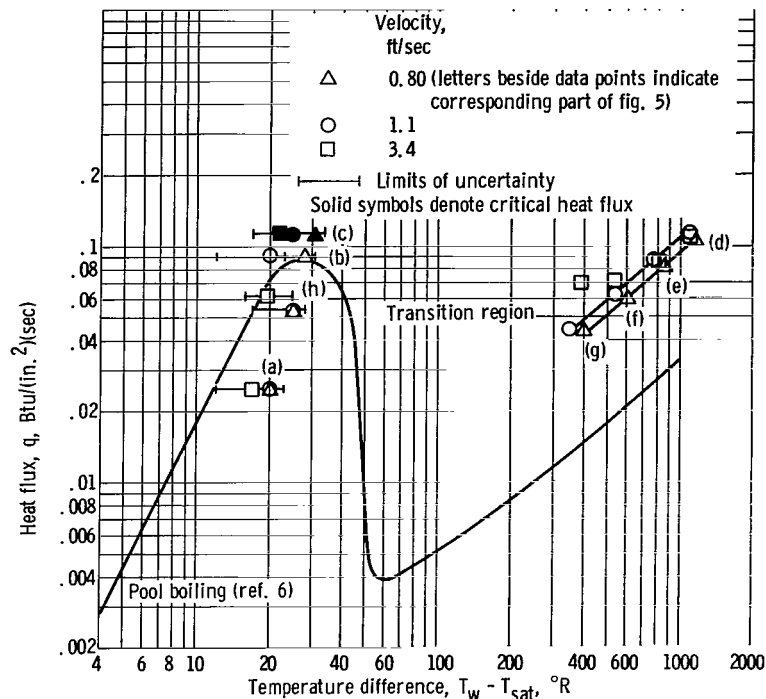
Figure 4. - Boiling curve of low-velocity liquid nitrogen. Pressure, 35 pounds per square inch absolute.

0.020-in. max. diam) discrete bubbles give way at higher heat fluxes to much larger (0.150-in. diam) coalitions of bubbles. These large, coalesced vapor masses tend to become elongated, and although there is considerable jetting into the stream, much of the vapor remains pressed against the wall. This behavior is consistent with observations of reference 3 concerning the condition of water vapor as the critical heat flux is approached. The photographic sequence in figure 5 suggests that an increase in power will increase the trajectory angle of the bubbles. For low power, the bubbles rise vertically (no trajectory), while the initial trajectory is almost horizontal near the critical heat flux.

Figures 5(d) to (g) represent a decrease in power in the film-boiling regime from a heat-flux level, which is equal to the critical heat flux, to the minimum heat flux. The minimum heat flux occurs when the vapor film collapses and nucleate boiling becomes the mode of heat transfer. Heat fluxes for 85, 60, 45, and 35 percent of the critical heat flux are shown in figures 5(d), (e), (f), and (g), respectively. It should be noted that, as the power is decreased, the randomness of the vapor generation gives way to a more regular wavelike behavior. Even at the higher power, however, the vapor does seem to come off the wall in a periodic manner. The accumulation decreases with decreased power. There seems to be a large net vapor generation, even though the bulk fluid is subcooled 6° to 10° R. As the minimum heat flux is approached, it is possible to achieve a condition where both nucleate and film boiling can occur along the strip (fig. 5(g)).
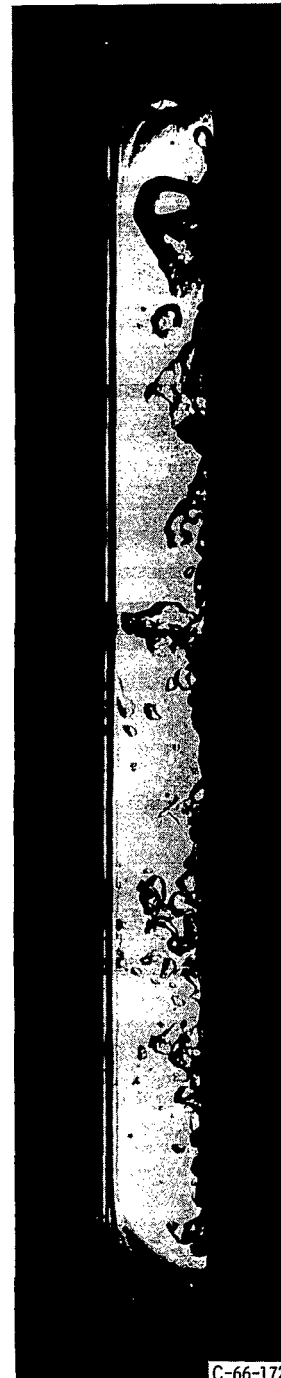
8
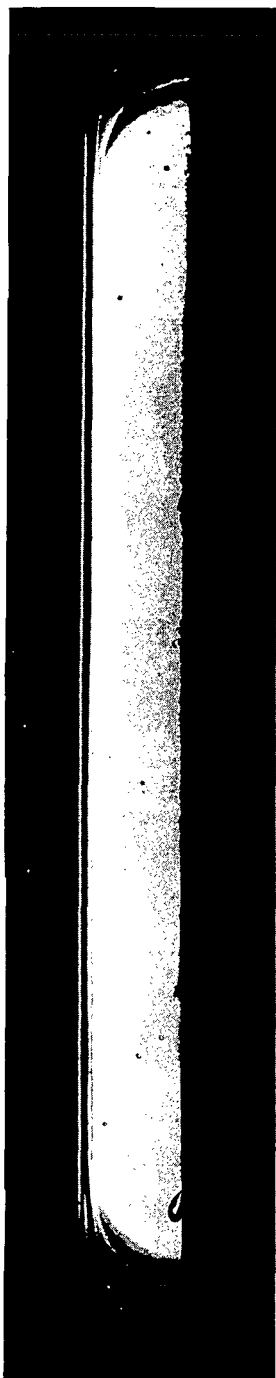
(a) Nucleate boiling. Heat flux, 0.025 Btu per square inch per second; 20 percent of critical heat flux.
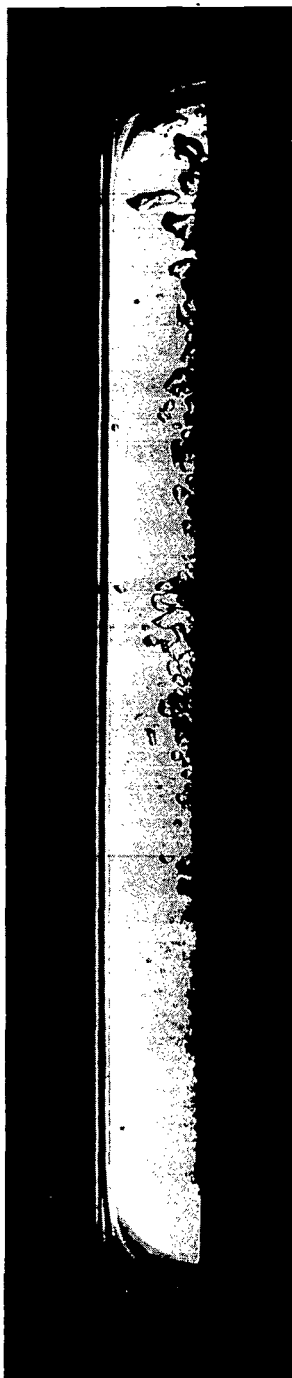
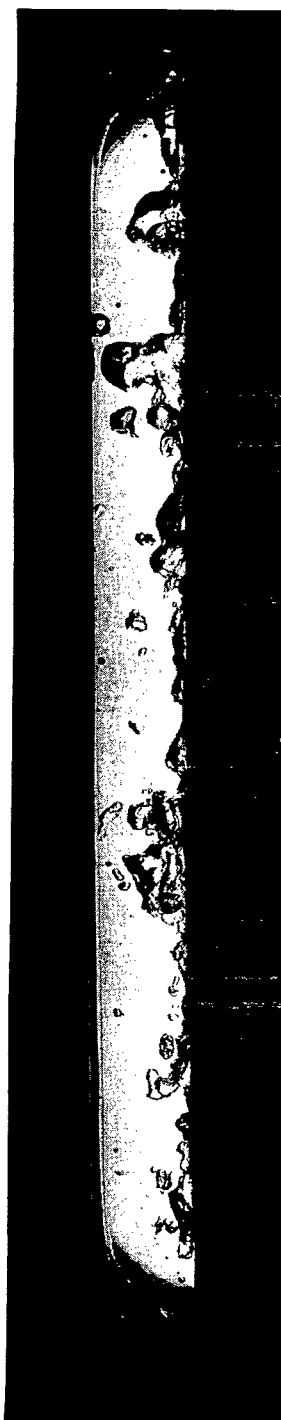(b) Nucleate boiling. Heat flux, 0.089 Btu per square inch per second; 70 percent of critical heat flux.
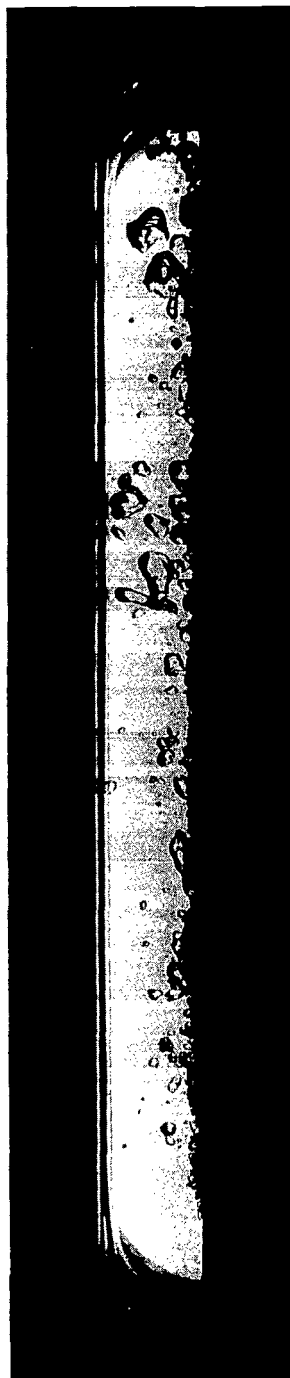
(c) Nucleate boiling. Heat flux, 0.11 Btu per square inch per second; 85 percent of critical heat flux.
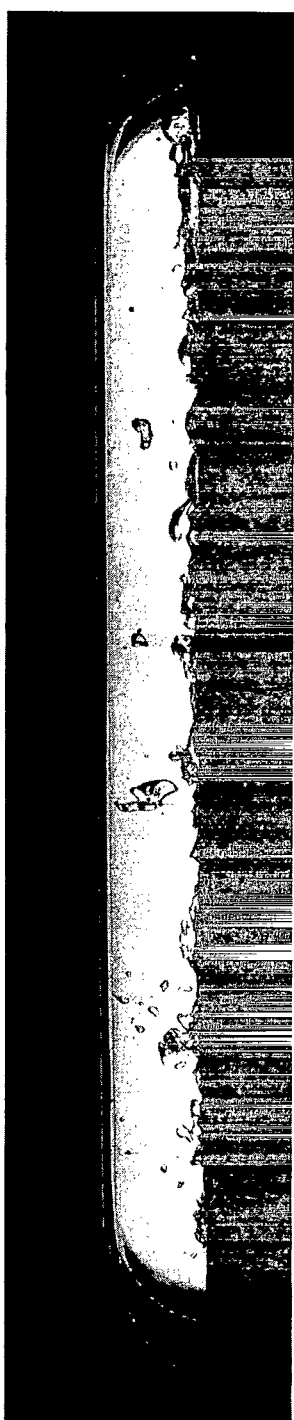
(d) Film boiling. Heat flux, 0.11 Btu per square inch per second; 85 percent of critical heat flux.
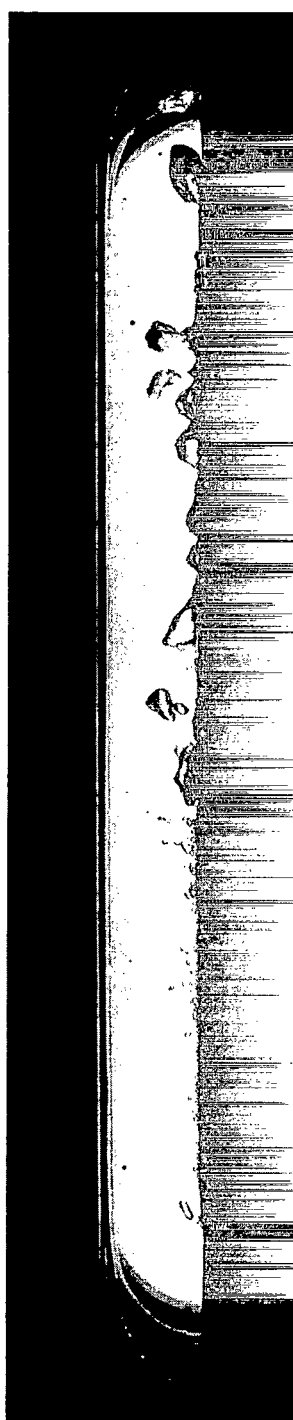
C-66-172

Figure 5. – Survey of boiling curve for low-velocity upward flow. Velocity, 0.80 foot per second.
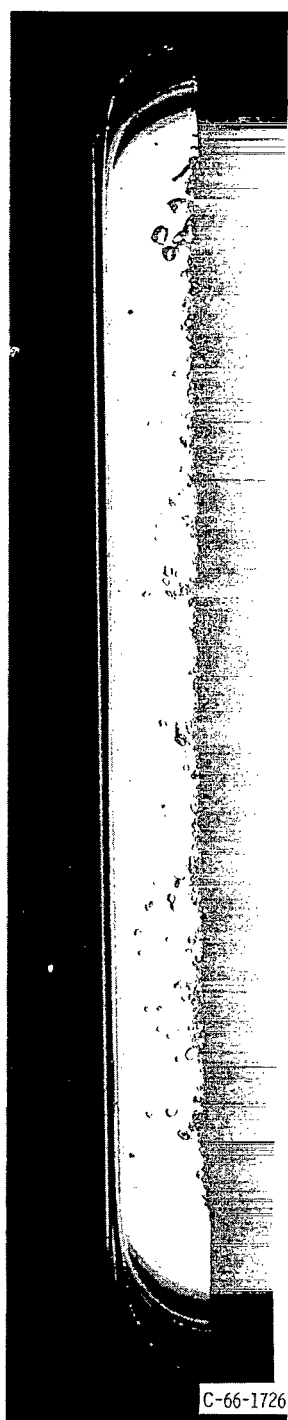
9

(e) Film boiling. Heat flux, 0.081 Btu per square inch per second; 60 percent of critical heat flux.

(f) Film boiling. Heat flux, 0.059 Btu per square inch per second; 45 percent of critical heat flux.

(g) Nucleate-boiling - film-boiling transition region. Heat flux, 0.043 Btu per square inch per second; 35 percent of critical heat flux.

(h) Nucleate boiling. Heat flux, 0.053 Btu per square inch per second; 40 percent of critical heat flux.

C-66-1726

Figure 5. - Concluded.

This condition is called the nucleate-film transition region. Figure 5(h) is a completion of the cycle back to total nucleate boiling.

NUCLEATE REGION OF HEATER B

In order to examine the effect of buoyancy and velocity in the nucleate regime, an intermediate level constant heat flux of 0.062 Btu per square inch per second is selected (fig. 6), which is about 70 percent of the critical heat flux. In figures 6(a) and (b), the flow is upward, while in figures 6(c) and (d), the flow is downward. Two velocity conditions are compared, 0.86 foot per second and a higher value of 2.6 feet per second.

Comparison of figures 6(a) and (c) shows the effect of body-force orientation on low-velocity flow. The vapor accumulation in the downward flow is significantly greater than in the upward flow at this low velocity. The vapor accumulation in downward flow was caused by bubbles that initially attempted to move upward against the flow direction and then finally move with the flow as they enter into the mainstream. Thus, a low bubble transport rate was created away from the heating surface, and bubble population or vapor accumulation was increased. Increasing the velocity to 2.6 feet per second (fig. 6(d)) tends to reduce the buoyancy effect. Comparing the flow on the left side of the heater in figure 6(b) to the same position in figure 6(d) shows only slightly more accumulation in the downward flow. To the right of the heater in figure 6(d) a very large vapor mass can be seen. The lowest electrode causes a low-velocity or stagnation region on the right side. The opposing buoyancy force has overcome inertia on the right but not on the left. The excess accumulation produces an artificially low critical heat flux. Comparing the right and left sides yields a rather graphic representation of the effect that liquid velocity has on vapor buoyancy. It should be noted that when the two forces are in the same direction (fig. 6(b)), this does not occur.

Finally, in the nucleate region, a buoyancy effect can be seen in the critical heat fluxes, which are given for heater A in table I. The critical heat flux for downward flow is lower than that for upward flow. Since figure 6 indicates greater accumulation in downward flow than in upward flow, this lower critical heat flux suggests that vapor accumulation is important in determining the critical heat flux in vertical flow systems.

TABLE I. - HEATER A - CRITICAL HEAT FLUXES

Heat flux, q (1 Btu/(in.^{2})(sec) = 1.634×10^6 W/m^2)	Flow rate, $\dot{w}$ (1 lb mass/sec = 0.454 kg mass/sec)	Velocity, V, ft/sec	Flow direction
0.117	0.279	0.81	Up
.128	.268	.81	
.140	.374	1.13	
.121	.293	3.46	
.101	.288	.84	Down
.107	.295	3.41	Down

(a) Low-velocity upward flow.   (b) Higher velocity upward flow.   (c) Low-velocity downward flow.   (d) Higher velocity downward flow.
Velocity, 0.86 foot per second.   Velocity, 2.6 feet per second.   Velocity, 0.87 foot per second.   Velocity, 2.6 feet per second.

Figure 6. - Comparison of velocity and body-force orientation effects on nucleate boiling. Heat flux, 0.062 Btu per square inch per second, 70 percent of critical heat flux.

(a) Upward flow.   (b) Downward flow.

Figure 7. – Effect of body-force orientation on low-velocity film boiling. Velocity, 0.85 foot per second; heat flux, 0.098 Btu per square inch per second.

FILM-BOILING REGIME

OF HEATER B

The effects of body-force orientation and velocity on boiling in the film region seem to be of the same general type as in the nucleate region. Figure 7 illustrates rather graphically the buoyancy effect on the lower velocity (0.85 ft/sec) flow. In figure 7(a), for upward flow, the boiling appears irregular; however, it is not nearly as irregular as it is for downward flow (fig. 7(b)). The really striking comparison is the vapor accumulation. In the downward flow, the vapor practically blocks the channel. In the motion pictures, it can actually be seen to move upward against the flow and form circulation patterns. Figure 8 shows some evidence of the effect of increasing the velocity to 2.5 feet per second; however, figures 7 and 8 cannot be compared exactly, because the heat fluxes are not the same (0.098 and 0.12 Btu/(in.^{2})(sec), respectively).

The increased velocity has diminished considerably the buoyancy effect. On the left side of the heater strip (fig. 8), the flow patterns appear quite similar. On the right side in downward flow, the large mass of vapor is the same as the mass that appeared in nucleate boiling (fig. 6(d)). Although this mass of vapor detracts from the comparison between upward and downward flows (fig. 8), it is

(a) Upward flow.   (b) Downward flow.

Figure 8. - Effect of body-force orientation on high velocity film boiling. Velocity, 2.6 feet per second; heat flux, 0.12 Btu per square inch per second.

useful in comparing the inertial force with the buoyancy force. This region is a stagnation region because the electrode is located in the flow path. By comparing the left and right sides of the flow in figure 8(b) it can be seen that inertia is counteracting the effect of the buoyancy force. For upward flow (fig. 8(a)), little increased accumulation is apparent in the same low-velocity region since the buoyancy and velocity forces are in the same direction.

Buoyancy effect on minimum heat flux. - Figure 9 illustrates some hydrodynamic effects of buoyancy and velocity on the minimum heat-flux condition. The conditions of figure 9 are not the minimum heat fluxes, but rather some point near the minimum; thus, only qualitative remarks can be made. Little noticeable hydrodynamic difference is apparent in the transition region with velocity (figs. 9(a) and (b)). When the flow is reversed to downward (figs. 9(c) and (d)), some striking buoyancy effects appear. For lower velocity (fig. 9(c)), the vapor is quite successful in rising against the flow. In addition, a deficiency of vapor near the downstream electrode permits nucleate boiling to appear. Thus, the unique situation arises of nucleate boiling at each end of a constant-heat-flux flow system with film boiling in the middle. As the velocity is increased (fig. 9(d)), the liquid drag is great enough to force the vapor down in the direction of flow.
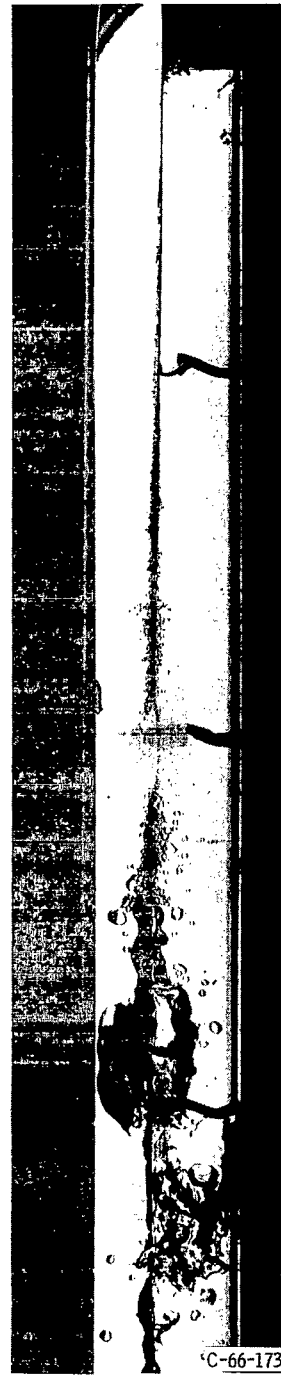
14

(a) Low-velocity upward flow. Velocity, 0.88 foot per second; heat flux, 0.042 Btu per square inch per second.

(b) Higher velocity upward flow. Velocity, 2.5 feet per second; heat flux, 0.034 Btu per square inch per second.

(c) Low-velocity downward flow. Velocity, 0.86 foot per second; heat flux, 0.042 Btu per square inch per second.

(d) Higher velocity downward flow. Velocity, 2.4 feet per second; heat flux, 0.031 Btu per square inch per second.

C-66-1730

Figure 9. - Effect of velocity and body-force orientation in vicinity of minimum heat flux.
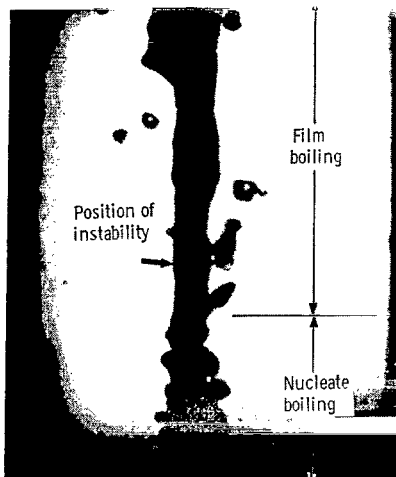
STABILITY DATA

High-speed motion pictures were taken of the region where nucleate and film boiling coexist in the vicinity of the minimum heat flux. This region is designated the nucleate-film transition region. Small capillary waves at the vapor-liquid interface were observed to grow in amplitude and become unstable, which caused the interface to be unstable and the film thickness at any position to be a function of time. The production of waves at the surface of a liquid by a gas stream was the subject of the work of Helmholtz (ref. 7) and Kelvin (ref. 8). Essentially, their theory predicts a minimum velocity difference between liquid and gas streams necessary for a capillary wave to grow undamped with time. The effect of a solid boundary was analyzed by Milne-Thomson (ref. 9), and the results were used by Rankin (ref. 10) in the study of film-boiling stability. Rankin's use of the stability theory for film boiling was limited because of the lack of wavelength data for capillary waves. This report presents wavelength data and provides visual evidence of the nature of the instability.

Figure 10 is a photographic enlargement (×20) of the transition region. Small capillary waves may be seen at the vapor-liquid interface. The average wavelength λ is 0.020 inch, and the liquid velocity is 0.88 foot per second. Figure 10 corresponds to the initial growth period when the waves first became evident. The motion pictures indicate that the mean thickness of the film grows with time (as the interface becomes unstable) and that the wavelength increases slightly as the amplitude increases; thus, the value of λ of 0.020 inch is probably slightly higher than the initial disturbance wavelength.

Figure 11 is a sequence of motion-picture frames that shows the nature and development of the instability. The conditions for upward flow are a velocity of 2.5 feet per second and a heat flux of 0.04 Btu per square inch per second. The first frame (fig. 11(a)) is the completion of a previous instability and is arbitrarily marked zero time for reference. In figure 11(b), the liquid-vapor interface appears smooth with no waves. This condition is of interest, since it occurs either prior to the initial perturbation or at a time when the perturbation is too small to be visible. At this condition, a minimum film thickness h_{min} with no disturbances is measured. A number of measurements of h_{min} were made from this motion picture, and the results were fairly constant. For the conditions of figure 11, h_{min} was 0.009 to 0.010 inch, and the average length of a stable vapor-liquid interface was 0.15 inch. Since the wavelengths grow as the instability progresses (figs. 11(a) to (g)), the wavelength measurement should be made as soon as the waves appear, which is approximately the condition shown in figure 11(b). As a practical point, the waves were measured as soon as the amplitudes were large enough to make them distinguishable. The wavelengths for the conditions just mentioned were also measured from the same motion picture. The wavelength measurements for 34 cycles of instability were found to have a distribution of about an average value of $\lambda = 0.04$ inch
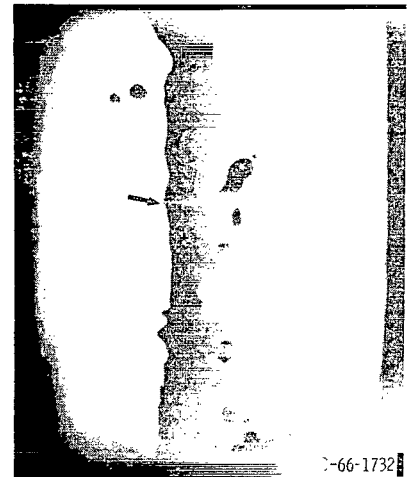
Waves

C-66-1731

Figure 10. - Nucleate transiton region in vicinity of minimum film-boiling heat flux (upward flow). Velocity, 0.88 foot per second; heat flux, 0.042 Btu per square inch per second.
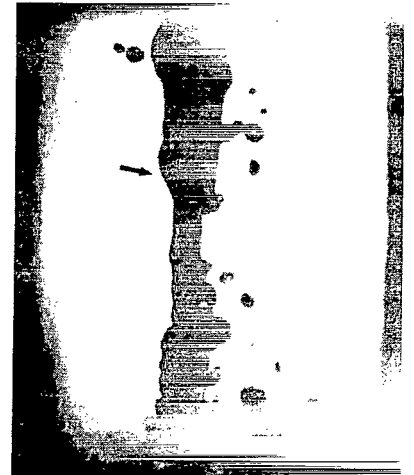
17

(a) 0.0 Second.

(b) 0.0008 Second.

(c) 0.0016 Second.

(d) 0.0022 Second.

(e) 0.0028 Second.

(f) 0.0034 Second.

(g) 0.0042 Second.

(h) 0.0054 Second.

Figure 11. - Nature of the hydrodynamic instability (upward flow). Velocity, 2.5 feet per second, heat flux, 0.04 Btu per square inch per second.
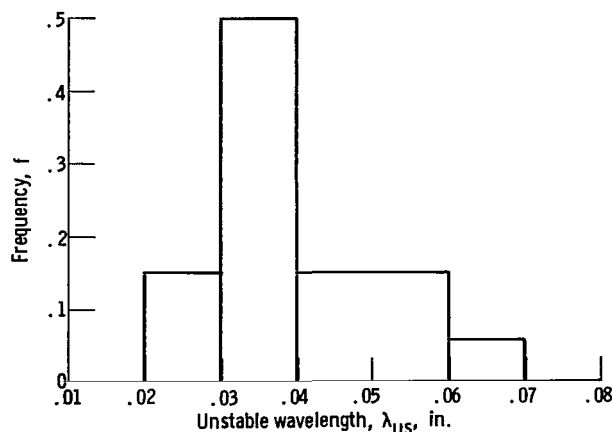
Figure 12. - Unstable wavelength distribution. Heat flux, 0.04 Btu per square inch per second; liquid velocity, 2.5 feet per second.

(fig. 12). Similar measurements were made from a motion-picture sequence in which the liquid velocity was 0.87 foot per second. Although the data were less extensive, a film thickness of 0.004 inch and an average wavelength of 0.016 inch were measured. Greater confidence can be given to the wavelength measurement because it is not subject to error from camera misalinement, while the film thickness could be. The results of these measurements suggest that, for this system of liquid nitrogen flowing upward across a heated strip, the following relation exists between the most unstable wavelength and film thickness:

$$\lambda_{us} = 4\ h_{min}$$

Although heater B was used for the measurements, the influence of the electrodes seemed to be small for two reasons: the measurements were made in a small region (less than 1/2 in.) near the middle of the strip away from the electrodes, and more important, only the upward-flow condition was used.

SUMMARY OF RESULTS

The results of a visual study of the velocity and buoyancy effects on boiling nitrogen can be summarized as follows:

1. For low-velocity upward flow, the boiling curve is similar to the pool-boiling curve. This statement is true at least if the heated- to-nonheated-surface-area ratio is small.

2. In both nucleate and film boiling in low-velocity vertical flow, velocity and buoyancy are important interrelated parameters. Particularly, vapor accumulation is affected, and, in the nucleate region, bubble trajectory is affected. Large vapor accumu-

19

lation occurs in both boiling regimes even though the main stream is subcooled 6° to 10°.

3. The body-force orientation effect on vapor accumulation, in turn, affects the critical heat flux. In low-velocity downward flow, the critical heat flux is lower than it is in low-velocity upward flow.

4. Measurements indicated that, for the film boiling of liquid nitrogen flowing upward over a flat surface, there exists a relation for the vapor-liquid interface between the most unstable wavelength and the film thickness so that the most unstable wavelength is four times the film thickness.

Lewis Research Center,
    National Aeronautics and Space Administration,
        Cleveland, Ohio, April 18, 1966.

REFERENCES

1. Dougall, Richard S.; and Rohsenow, Warren M.: Film Boiling on the Inside of Vertical Tubes with Upward Flow of the Fluid at Low Qualities. Tech. Rept. No. 9079-26, Massachusetts Inst. Tech., Sept. 1963.

2. Hsu, Yih Yun; and Graham, Robert W.: A Visual Study of Two-Phase Flow in a Vertical Tube with Heat Addition. NASA TN D-1564, 1963.

3. Kirby, G. J.; Staniforth, R.; and Kinneir, J. H.: A Visual Study of Forced Convection Boiling, Part I, Results for a Flat Vertical Heater. Rep. No. AEEW R-281, United Kingdom Atomic Energy Authority, Mar. 1965.

4. Griffith, Peter; Clark, John A.; and Rohsenow, Warren M.: Void Volumes in Subcooled Boiling Systems. Tech. Rep. no. 12, Massachusetts Inst. Tech., Mar. 1958.

5. Tippets, F. E.: Critical Heat Flux and Flow Pattern Characteristics of High Pressure Boiling Water in Forced Convection. Rep. No. GEAP 3766, General Electric Atomic Power Equipment Dept., Apr. 1962.

6. Merte, H.; and Clark, J. A.: Boiling Heat-Transfer Data for Liquid Nitrogen at Standard and Near-Zero Gravity. Vol. 7 of Advances in Cryogenic Engineering, K. D. Timmerhaus, ed., Plenum Press, 1962, pp. 546-550.

7. Chandrasekhar, S.: Hydrodynamic and Hydromagnetic Stability. Clarendon Press, Oxford, 1961, ch. 11, p. 512, ref. 3. (H. Helmholtz: 'Ueber discontinuirliche Flussigkeitsbewegungen', Berl, Monatsber, Apr. 1868; Wissenschaftliche Abhandlungen, 146-57, J. A. Barth, Leipzig, 1882; translation by Guthrie in Phil. Mag., Ser. 4, 36, 337-46 (1868).)

8. Chandrasekhar, S.: Hydrodynamic and Hydromagnetic Stability. Clarendon Press, Oxford, 1961, ch. 11, p. 512, ref. 4, (Lord Kelvin, 'Hydrokinetic Solutions and Observations,' 'On the Motion of Free Solids Through a Liquid, 69-95,' 'Influence of Wind and Capillarity on Waves in Water Supposed Frictionless, 76-85', Mathematical and Physical Papers, 9iv, Hydrodynamics and General Dynamics, Cambridge, England, 1910.)

9. Milne-Thomson, Louis M.: Theoretical Hydrodynamics. 4th ed., St. Martin's Press, New York, 1960, p. 409.

10. Rankin, S.: Heat Transfer to Boiling Liquids Under Conditions of High Temperature Difference and Forced Convection. Rep. No. UD-FB-13, University of Delaware, Feb. 1958.

A motion-picture film supplement C-245 is available on loan. Request will be filled in the order received. You will be notified of the approximate date scheduled.

The film (16 mm, 17 min, color, sound) shows nucleate and film boiling in low-velocity flowing nitrogen, with buoyancy acting with and in opposition to the liquid velocity. A detailed view of film boiling instability is included.

Film supplement C-245 is available on request to:

Chief, Technical Information Division (5-5)
National Aeronautics and Space Administration
Lewis Research Center
21000 Brookpark Road
Cleveland, Ohio, 44135

- CUT - - - - - - - -

Date _____

Please send, on loan, copy of film supplement C-245 to
TN D-

Name of organization _____

Street number _____

City and State _____ Zip code _____

Attention: Mr. _____
              Title _____

"The aeronautical and space activities of the United States shall be conducted so as to contribute . . . to the expansion of human knowledge of phenomena in the atmosphere and space. The Administration shall provide for the widest practicable and appropriate dissemination of information concerning its activities and the results thereof."

—NATIONAL AERONAUTICS AND SPACE ACT OF 1958

NASA SCIENTIFIC AND TECHNICAL PUBLICATIONS

TECHNICAL REPORTS: Scientific and technical information considered important, complete, and a lasting contribution to existing knowledge.

TECHNICAL NOTES: Information less broad in scope but nevertheless of importance as a contribution to existing knowledge.

TECHNICAL MEMORANDUMS: Information receiving limited distribution because of preliminary data, security classification, or other reasons.

CONTRACTOR REPORTS: Technical information generated in connection with a NASA contract or grant and released under NASA auspices.

TECHNICAL TRANSLATIONS: Information published in a foreign language considered to merit NASA distribution in English.

TECHNICAL REPRINTS: Information derived from NASA activities and initially published in the form of journal articles.

SPECIAL PUBLICATIONS: Information derived from or of value to NASA activities but not necessarily reporting the results of individual NASA-programmed scientific efforts. Publications include conference proceedings, monographs, data compilations, handbooks, sourcebooks, and special bibliographies.

Details on the availability of these publications may be obtained from:

SCIENTIFIC AND TECHNICAL INFORMATION DIVISION

NATIONAL AERONAUTICS AND SPACE ADMINISTRATION

Washington, D.C. 20546